

ORIGINAL ARTICLE

PHOSPHATE exporter XPR1/SLC53A1 is required for the tumorigenicity of epithelial ovarian cancer

Yoko Akasu-Nagayoshi^{1,2} | Tomoatsu Hayashi¹  | Ayako Kawabata^{1,2} | Naomi Shimizu¹ | Ai Yamada¹ | Naoko Yokota³ | Ryuichiro Nakato³ | Katsuhiko Shirahige⁴ | Aikou Okamoto² | Tetsu Akiyama¹ 

¹Laboratory of Molecular and Genetic Information, Institute for Quantitative Biosciences, The University of Tokyo, Tokyo, Japan

²Department of Obstetrics and Gynecology, Jikei University School of Medicine, Tokyo, Japan

³Laboratory of Computational Genetics, Institute for Quantitative Biosciences, The University of Tokyo, Tokyo, Japan

⁴Laboratory of Genome Structure and Function, Institute for Quantitative Biosciences, The University of Tokyo, Tokyo, Japan

Correspondence

Tomoatsu Hayashi and Tetsu Akiyama, Laboratory of Molecular and Genetic Information, Institute for Quantitative Biosciences, The University of Tokyo, 1-1-1 Yayoi, Bunkyo-ku, Tokyo, 113-0032, Japan.

Emails: hiroton-h@iqb.u-tokyo.ac.jp(T.H.); akiyama@iqb.u-tokyo.ac.jp(T.A.)

Funding information

Project for Cancer Research and Therapeutic Evolution (P-CREATE), Grant/Award Number: 17cm0106103h0002; Japan Agency for Medical Research and Development; Ministry of Education, Culture, Sports, Science and Technology of Japan, Grant/Award Number: 17H06325; Japan Society for the Promotion of Science, Grant/Award Number: 21K07146

Abstract

Ovarian cancer is the fifth most common cause of cancer-related death in women. Ovarian clear cell carcinoma (OCCC) is a chemotherapy-resistant epithelial ovarian cancer with poor prognosis. As a basis for the development of therapeutic agents that could improve the prognosis of OCCC, we performed a screen for proteins critical for the tumorigenicity of OCCC using the CRISPR/Cas9 system. Here we show that knockdown of the phosphate exporter XPR1/SLC53A1 induces the growth arrest and apoptosis of OCCC cells in vitro. Moreover, we show that knockdown of XPR1/SLC53A1 inhibits the proliferation of OCCC cells xenografted into immunocompromised mice. These results suggest that XPR1/SLC53A1 plays a critical role in the tumorigenesis of OCCC cells. We speculate that XPR1/SLC53A1 might be a promising molecular target for the therapeutic treatment of OCCC.

KEYWORDS

apoptosis, ovarian cancer, phosphate transporter, proliferation, tumorigenicity, XPR1

Abbreviations: ARID1A, AT-rich interaction domain 1A; CRISPR/Cas9, clustered regularly interspaced short palindromic repeat/CRISPR associated protein 9; GADD45A, growth arrest and DNA damage inducible alpha; GO, Gene Ontology; GSEA, Gene Set Enrichment Analysis; GTEx, genotype tissue expression; K-ras, KRAS proto-oncogene GTPase; MAGECK, model-based analysis of genome-wide CRISPR-Cas9 knockout; NOXA, phorbol-12-myristate-13-acetate-induced protein 1; OCCC, ovarian clear cell carcinoma; p53, tumor protein P53; PIK3CA, phosphatidylinositol-4,5-bisphosphate 3-kinase catalytic subunit alpha; PUMA, p53 upregulated modulator of apoptosis; sgRNA, single-guide RNA; TKO, Toronto Knockout; XPR1/SLC53A1, xenotropic and polytropic retrovirus receptor 1/solute carrier 53A1.

This is an open access article under the terms of the [Creative Commons Attribution-NonCommercial](https://creativecommons.org/licenses/by-nc/4.0/) License, which permits use, distribution and reproduction in any medium, provided the original work is properly cited and is not used for commercial purposes.

© 2022 The Authors. *Cancer Science* published by John Wiley & Sons Australia, Ltd on behalf of Japanese Cancer Association.

1 | INTRODUCTION

Epithelial ovarian cancer has one of the worst prognoses among gynecologic malignancies.^{1,2} Approximately 60% of epithelial ovarian cancer cases are diagnosed at stages III and IV, and their 5-year survival rate is less than 30%.^{3,4} Epithelial ovarian cancer is classified into four major histological subtypes: serous, clear cell, endometrioid, and mucinous.⁵ Ovarian clear cell carcinoma is less sensitive to conventional platinum-based chemotherapy and has worse prognosis than other subtypes.^{6–10} The incidence of OCCC in ovarian cancer is higher in Asia, especially in Japan (25% of ovarian cancers), than in North America and Australia (5%).^{11,12} Mutations in various oncogenes and tumor suppressor genes, including *K-ras*, *p53*, *ARID1A*, and *PIK3CA*, have been shown to be involved in the development of OCCC.^{13,14} In particular, *ARID1A* and *PIK3CA* are mutated in approximately half of the cases of OCCC.

Human xenotropic and polytropic retrovirus receptor 1/solute carrier 53A1 (hereafter called XPR1) was originally identified as a receptor for xenotropic and polytropic murine leukemia viruses.^{15–17} As a multipass transmembrane protein, XPR1 functions as an inorganic phosphate exporter.¹⁸ In cooperation with the phosphate importer SLC20A2, XPR1 regulates cellular phosphate homeostasis in an inositol polyphosphate-dependent manner: inositol pyrophosphate (PP-InsP) signaling molecules such as 1,5-bis-diphosphoinositol 2,3,4,6-tetrakisphosphate (InsP₈) interact with the N-terminal SYG1-Pho81-XPR1 (SPX) domain of XPR1 and regulate its phosphate exporter activity.^{19,20} In addition, XPR1 has been reported to regulate cAMP levels through an interaction with G protein β subunits, although its role in phosphate regulation remains to be elucidated.²¹ Mutations in XPR1 have been identified in patients with primary familial brain calcification, a genetic disease characterized by cerebral calcium phosphate deposition and associated with neuropsychiatric disorders.^{22,23} Furthermore, it has been reported that XPR1 expression is enhanced in tongue squamous cell carcinoma tissues compared to normal tongue tissues and correlates with poor prognosis.²⁴

We attempted to identify novel molecular targets critical for the proliferation and tumorigenicity of OCCC using the CRISPR/Cas9 system. In this study, we show that the phosphate exporter XPR1 plays an important role in the proliferation and tumorigenicity of OCCC.

2 | MATERIALS AND METHODS

2.1 | Cell culture

Human ovarian cancer OVISE and JHOC5 cells were cultured in DMEM and RPMI-1640 medium (Nissui) supplemented with 10% FBS, respectively. TOV21G cells were cultured in MCDB 105 (50%)/Medium 109 (Sigma) supplemented with 10% FBS. ES2, HCT116 (p53^{+/+}), and HCT116 (p53^{-/-}) cells were grown in McCoy 5A (Sigma) supplemented with 10% FBS.

2.2 | CRISPR-CAS9 screening

CRISPR-CAS9 screening was carried out using TKO CRISPR Library Version 3 (lentiCRISPRv2; Addgene #90294) following the protocols provided in <https://www.addgene.org/pooled-library/moffat-crispr-knockout-tkov3/>.²⁵ The OCCC cell lines OVISE, ES2, TOV21G, and JHOC5 were transfected with lentiCRISPRv2 at an MOI of 0.3 followed by selection with puromycin for 2 days. A sample of 2×10^7 cells was then pelleted and frozen under liquid nitrogen as a Day 0 sample. Cells were then passaged until they had undergone eight doublings. To maintain sufficient sgRNA coverage, the total number of cells was maintained above 2×10^7 for the duration of the culture period. Cells cultured for eight cell doublings from Day 0 were taken as a final time point. Genomic DNA was extracted using the Blood and Cell Culture DNA MidiKit (#13343; Qiagen). One hundred twenty five micrograms of genomic DNA from each sample was split into 2.5 μ g fractions and sgRNA sequences were amplified using Herculase II fusion DNA polymerase. Reactions were measured for fragment size using the Agilent 2200 TapeStation and quantified using the KAPA SYBR Fast qPCR Kit (#7959362001; KAPA Biosystems). To generate and analyze sgRNA count data, MAGeCK (version 0.5.9) was used (“mageck count” and “mageck mle --norm-method control --control-sgrna --cnv-norm” command).²⁶

2.3 | Small interfering RNA transfection

Silencer select siRNA targeting XPR1 was purchased from Ambion (siXPR1#1, #17614; siXPR1#2, #17615). Cells were transfected with siRNA using Lipofectamine RNAiMax (Thermo Fisher Scientific). Silencer select siRNA negative control (4390843; Thermo Fisher Scientific) was used as a control.

2.4 | Human ovarian cancer samples

Ovarian cancer tissues were prepared as described previously¹¹ according to the guidelines of the Declaration of Helsinki, and approved by the Ethics Committees of Jikei University School of Medicine and The Institute for Quantitative Bioscience, The University of Tokyo. Informed consent was obtained from all subjects involved in the study.

2.5 | RNA sequencing analysis

Total RNA was extracted using TRIreagent (Bioline). For ovarian cancer tissue dataset, cDNA libraries were prepared using the Illumina TruSeq Stranded Total RNA and the Ribo-Zero Gold LT Sample Prep Kit. All libraries were sequenced using an Illumina HiSeq 2500 to create single-end 65 bp reads, which were aligned to the human reference genome build hg38 using STAR.²⁷ For XPR1 knockdown dataset, sequencing library construction (mRNA-seq) and Illumina sequencing

(paired-end 150 bp reads) were undertaken by AnnoRoad Gene Technology. RSEM²⁸ was used to calculate transcripts per kilobase million (TPM, Ensembl gene annotation GRCh38). For differential expression analyses, we applied the count data to edgeR.²⁹ The count data were fitted with a general linear model. Gene Ontology enrichment analysis and GSEA were undertaken using the R package "clusterProfiler".³⁰ The ovarian normal tissue dataset from GTEx in UCSC Xena (<https://xena.ucsc.edu/>) was combined with our ovarian cancer tissue dataset (see above), and then normalized by the quantile method using the R package "limma".

2.6 | Cell viability assay

Cells (1×10^3 cells) were transfected with siRNA (10 nM) and seeded into 96-well plates. After 24 h, fresh medium was replaced. One, 4, and 6 days after transfection, cell viability was assessed indirectly by measuring the intracellular levels of ATP using the CellTiter-Glo Luminescent Cell Viability Assay kit (Promega). Luminescence was measured on a Mithras LB 940 (Berthold).

2.7 | Quantitative RT-PCR

Total mRNA was extracted using TRIsure (Bioline) and reverse-transcribed into cDNA using PrimeScript RT Master Mix (Takara). Real-time PCR was carried out using a LightCycler480 (Roche). The results were normalized against the values detected for GAPDH. Primers used for quantitative RT-PCR are described in Table S1.

2.8 | Immunoblotting

Immunoblotting analysis was carried out as described previously.³¹ Cells were lysed in RIPA buffer (50 mM Tris-HCl pH 8.0, 150 mM NaCl, 1.0% NP-40, 0.5% sodium deoxycholate, 0.1% SDS) and incubated at 37°C for 30 min, then separated by SDS-PAGE and probed with anti-XPR1 (14174-1-AP; Proteintech Group, Inc.), anti-p53 (sc-126; Santa Cruz Biotechnology), or anti-GAPDH (MAB374; EMD Millipore Corp.) Ab.

2.9 | Lentivirus production

Lentiviral vector (CS-Rfa-CG) harboring an shRNA driven by the H1 promoter was transfected with the packaging vectors (pMD2G, psPAX2; Addgene) into 293FT cells using polyethylenimine (Polysciences, Inc.). All plasmids were kindly provided by H. Miyoshi (Riken BioResource Center). Virus supernatants were purified by ultracentrifugation at 106, 800 \times g for 135 min (SW32Ti rotor; Beckman). Infection efficiency was monitored by GFP expression driven by the CMV promoter. The sequences of shRNAs are shown in Table S2.

2.10 | Mouse xenograft model

OVISe and ES2 cells infected with a lentivirus expressing an shRNA targeting XPR1 were injected s.c. into 7-week-old NOG mice (OVISe) and nude mice (ES2), respectively (NOD/Shi-scid IL-2R γ KO for OVISe, BALB/c-nu/nu for ES2; CLEA). Cells (1.0×10^6) for each injection were resuspended in a 1:1 mixture of 75 μ l PBS and 75 μ l Matrigel (Corning Life Sciences). All animal experimental protocols were carried out in accordance with the guidelines of the Animal Ethics Committee of the University of Tokyo.

2.11 | Sub-G₁ assays

Cells transfected with siRNA were cultured for 48 or 96 h, and fixed in a 70% ethanol : water solution at -30°C overnight. Fixed cells were incubated in a 4 mM citric acid (pH 8.0), 200 mM Na₂HPO₄ solution for 20 min, stained with a solution of 10 μ g/ml propidium iodide (Sigma) and 10 μ g/ml RNase A (Sigma) in 1 \times PBS for an additional 20 min, and subsequently analyzed on a Sony EC800 Flow Cytometry Analyzer.

2.12 | Statistical analysis

Statistical analyses, including unpaired t-tests and Wilcoxon test, were undertaken using R version 4.0.1 (<http://www.r-project.org/>).

3 | RESULTS AND DISCUSSION

3.1 | Genome-wide CRISPR/CAS9 screens using OCCC cell lines

To identify *genes* critical for the proliferation of OCCC, we previously performed CRISPR/CAS9 screens against the OCCC cell lines OVISe, ES2, TOV21G, and JHOC5 (Table 1) using the TKOv3 sgRNA library. From a list of *genes* selected in this screen (Data S1), we focused on *genes* that encode membrane proteins overexpressed in cancer cells, which could be suitable targets for Ab drug development. We observed that depletion of 22 *genes* encoding the SLC family of membrane proteins resulted in a significant decrease in the proliferation of OCCC cell lines (Figure 1A). Furthermore, we analyzed data from the Cancer Dependency Map (<https://depmap.org>) and found that depletion of SLC family *genes* such as PHC/

TABLE 1 Mutations in ovarian clear cell carcinoma cell lines

Cell line	Mutations
JHOC5	<i>TERT</i>
ES2	<i>TP53, BccF, JAK1</i>
OVISe	<i>PIK3CA, ARID1A, ARID1B, PPP2R1A, STAT3</i>
TOV21G	<i>PIK3CA, ARID1A, ARID1B, KRAS, PTEN, CTNNB1, JAK1</i>

SLC25A3 (mitochondrial phosphate and copper transporter), ZIP10/SLC39A10 (zinc transporter), MDU1/SLC3A2 (glutamate/cystine transporter), GLUT1/SLC2A1 (glucose transporter), and

XPR1/SLC53A1 (phosphate exporter) led to a prominent decrease in the growth of ovarian cancer cell lines, including OCCC cell lines (Figure 1B). Although PHC/SLC25A3 had a prominent effect on the

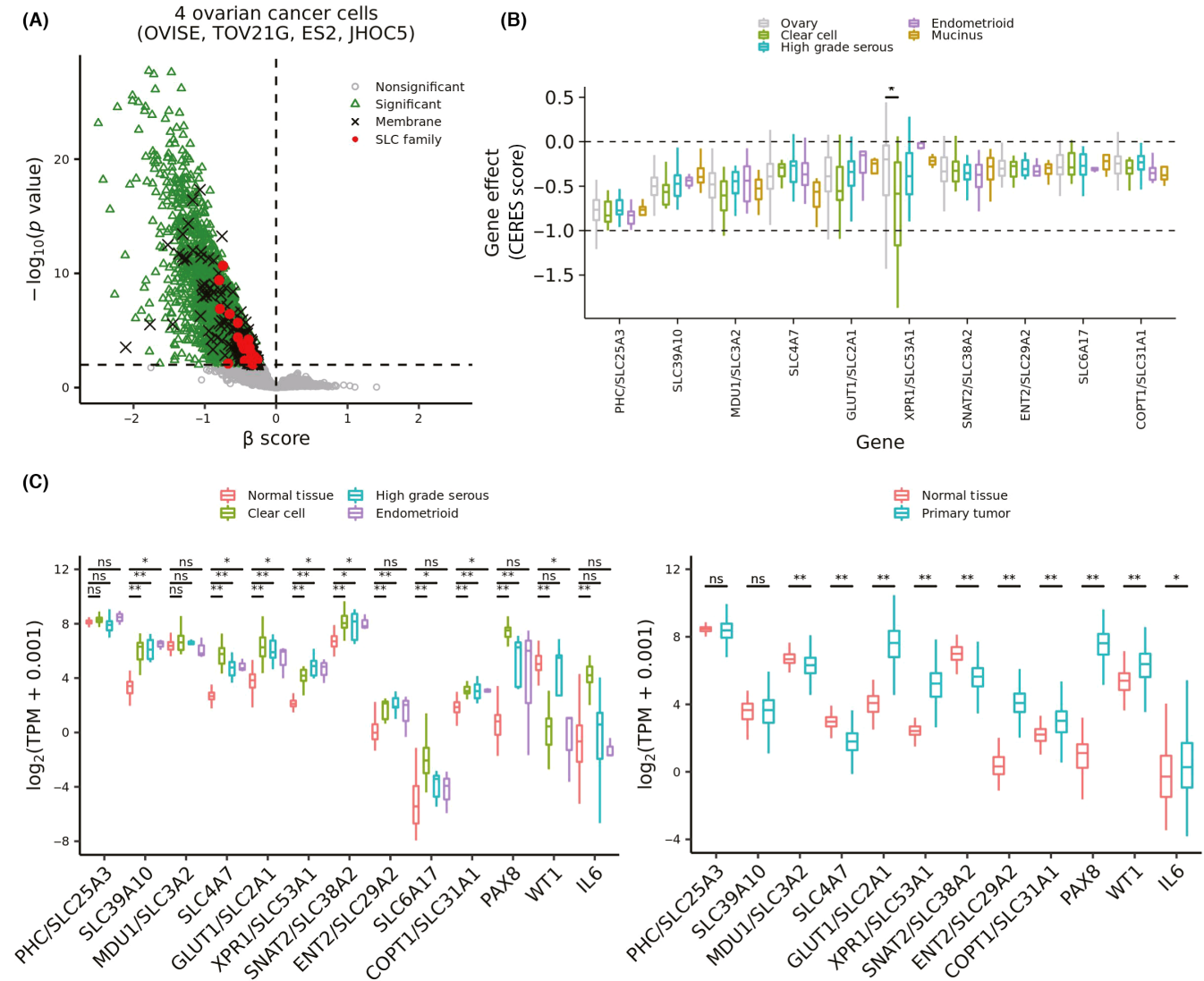
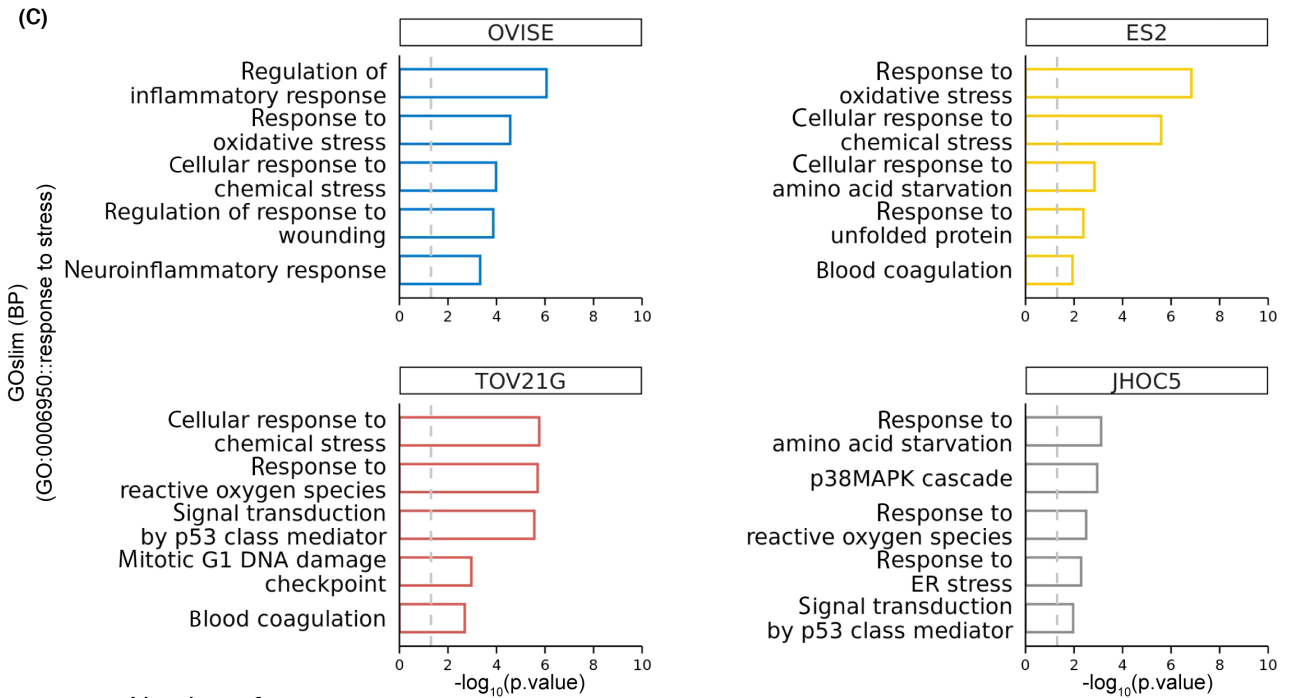
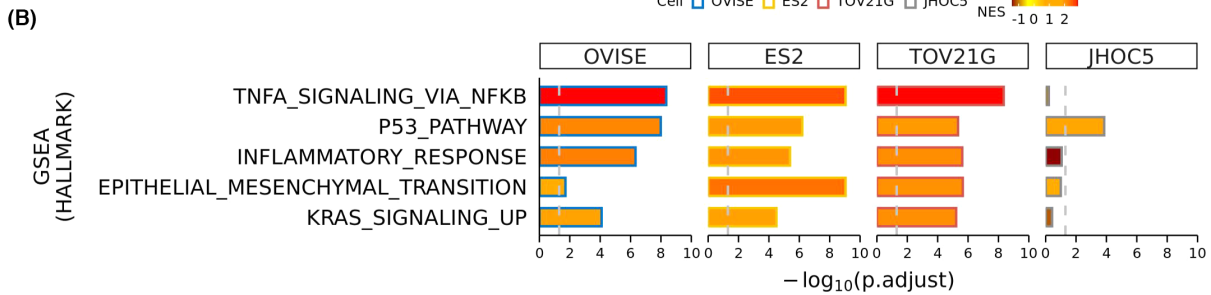
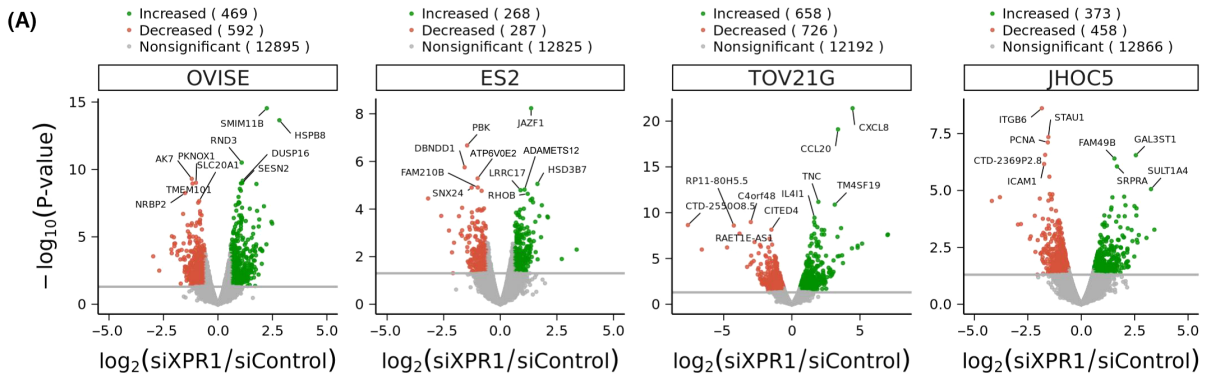
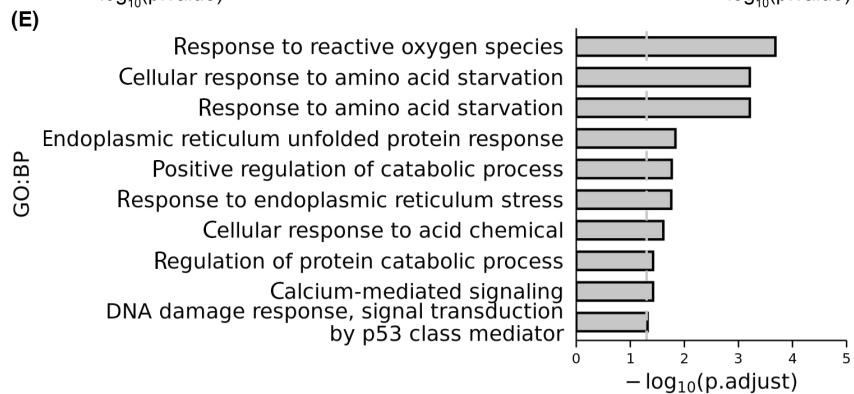
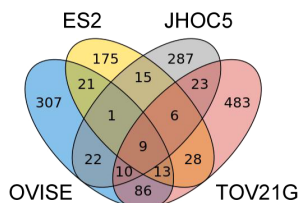


FIGURE 1 Genome-wide CRISPR/CAS9 screens using ovarian cancer cell lines. (A) Results of CRISPR/Cas9 screens against four types of ovarian cancer cell lines using the TKOv3 single guide RNA library. Green triangles indicate *genes* essential for growth in the four ovarian cancer cell lines ($p < 0.05$). Black crosses indicate *genes* encoding membrane proteins, and red circles indicate *genes* encoding the SLC family of membrane proteins. (B) Dependency of ovarian cancer cell lines on SLC family *genes* (data from <https://depmap.org>). A lower score means that a gene is more likely to be dependent in a given cell line. (C) Quantification of SLC gene family expression from RNA sequencing data. Left panel: normal tissue, $n = 200$ (from GTEx [genotype tissue expression]); clear cell carcinoma, $n = 11$; high grade serous adenocarcinoma, $n = 8$; endometrioid carcinoma, $n = 4$. Cancer tissues were prepared in our laboratory. Right panel: data of high grade serous adenocarcinoma from UCSC Xena (TCGA TARGET GTEx). PAX8, WT1, and IL6 are controls (PAX8 is known to be upregulated in ovarian cancer, WT1 is downregulated, and IL6 is upregulated in clear cell carcinoma). TPM, transcripts per million. * $p < 0.05$; ** $p < 0.01$. ns, not significant, Wilcoxon rank sum test

FIGURE 2 RNA sequencing (RNA-seq) analysis of ovarian clear cell carcinoma (OCCC) cell lines transfected with siRNA targeting XPR1. (A) Volcano plots of RNA-seq data obtained with OCCC cell lines transfected with control siRNA or siRNA targeting XPR1. *Genes* whose expression was significantly changed by XPR1 knockdown are shown in the volcano plots ($\log_{2}FC > 0.6$; $p \text{ value} < 0.05$). (B) Gene Set Enrichment Analysis (GSEA HALLMARKS) of RNA-seq data. Five terms common to two or more of the OCCC cell lines are shown. (C) Gene Ontology (GO) overrepresentation analysis of RNA-seq data in (A). The top five terms classified as response to stress in the Biological Process (BP) of GO-slim are shown for each cell line. (D) Venn diagram summarizing the number of *genes* upregulated by XPR1 knockdown. (E) BP analysis of GO for *genes* commonly upregulated in more than three cell lines (31 *genes* in (D))



(D) Number of upregulated genes in XPR1 knockdown cells



proliferation of most ovarian cancer cell lines, it is a mitochondrial protein that is not suitable for Ab drug development.³² Depletion of XPR1 led to a remarkable decrease in the growth of OCCC cell lines compared to other ovarian cancer cell lines. We next examined the expression levels of these SLC family members in ovarian cancers. We observed that ZIP10/SLC39A10, GLUT1/SLC2A1, and XPR1/SLC53A1, but not PHC/SLC25A3 or MDU1/SLC3A2, were upregulated in ovarian cancers compared to normal tissue (Figure 1C). As many studies have already been done on SLC39A10 and SLC2A1, we decided to focus on XPR1.

3.2 | Effect of XPR1 knockdown on gene expression profiles of OCCC cell lines

To clarify the effect of XPR1 knockdown on gene expression profiles of OCCC cells, we undertook RNA sequencing and GSEA using OVI5E, ES2, TOV21G, and JHOC5 cells transfected with siRNA targeting XPR1 (Figure 2A,B). The GSEA revealed that the p53 pathway was activated in all cell lines. Inconsistent with a previous report,²⁴ nuclear factor- κ B signaling was enhanced in OVI5E, ES2, and TOV21G cells. Inflammatory response, epithelial-mesenchymal transition, and K-ras signaling were also activated in all of these cell lines. Gene Ontology overrepresentation analysis revealed that expression of *genes* involved in oxidative stress and other stress responses was enhanced in all cell lines (Figure 2C). The GO biological process analysis indicated that the *genes* upregulated in common in at least three cell lines (Figure 2D) were enriched for those involved in stress response function (Figure 2E).

3.3 | Knockdown of XPR1 suppresses the growth of OCCC cells

We next attempted to examine the effects of RNAi-mediated knockdown of XPR1 on the growth and tumorigenicity of OCCC cells. As OVI5E and ES2, but not TOV21G or JHOC5, were tumorigenic in mice, we used OVI5E and ES2 in subsequent experiments. We found that siRNA knockdown of XPR1 resulted in a significant decrease in the proliferation of both cell lines in vitro (Figure 3A,B). Consistent with a previous report,¹⁸ the intracellular phosphate level was also decreased (Figure S1). Furthermore, FACS analysis revealed that knockdown of XPR1 induced the accumulation of sub-G₁ cells (Figure 3C). We therefore measured the changes in the expression of marker *genes* indicating p53-mediated apoptosis: *PUMA*, *NOXA*, and *GADD45*. Quantitative RT-PCR revealed that knockdown of XPR1 in OVI5E cells resulted in a marked increase in the expression of these marker *genes* (Figure 3D). However, knockdown of XPR1 in ES2 cells resulted in a smaller increase in marker expression. This result could be consistent with the fact that ES2 cells harbor a mutation in one allele of *p53*.

To further clarify the significance of *p53* in XPR1 knockdown-induced growth suppression, we compared the effects of siRNA against XPR1 on the proliferation of the colon tumor cell lines HCT116 (*p53*^{+/+}) and a derivative, HCT116 (*p53*^{-/-}), in which *p53* is disrupted by homologous recombination.³³ We found that knockdown of XPR1 caused both a marked inhibition of the proliferation and an increase in the sub-G₁ population of both cell lines (Figure 4A–D). However, knockdown of XPR1 induced upregulation of *PUMA*, *NOXA*, and *GADD45* only in HCT116 (*p53*^{+/+}) cells and not in HCT116 (*p53*^{-/-}) cells (Figure 4E). These results suggest that knockdown of XPR1 can suppress the proliferation of cancer cells through both *p53*-dependent and -independent mechanisms.

We next investigated the effects of siRNA-mediated knockdown of XPR1 on the growth of various cancer cell lines (Figures S2A,B). Immunoblotting analysis was also undertaken to examine XPR1 protein expression in these cell lines. We considered XPR1 to be three bands between 63 and 75 kDa (Figure S3A), because exogenously expressed XPR1 migrated to the same position (Figure S3B). Moreover, the intensity of these three bands was decreased in TOV21G cells transfected with siRNAs targeting XPR1 (Figure S3C). Furthermore, we examined the expression levels of XPR1 in various cancer tissues and corresponding normal tissues (Figure S4). For example: in lung cancer, XPR1 expression was higher than normal tissue and XPR1 knockdown was effective against H1299 but not A549 cells; in renal cancer, XPR1 expression was not much different from normal tissue, but XPR1 knockdown was effective against 786O cells; and in colon cancer, XPR1 knockdown was effective against HCT116 (Figure 4C) but not DLD1 cells. These results suggest that the sensitivity of cancer cells to XPR1 knockdown cannot simply be explained by XPR1 expression levels.

3.4 | Knockdown of XPR1 suppresses the tumorigenicity of OCCC cells

Finally, we examined the effects of an shRNA targeting XPR1 on the tumorigenicity of OCCC cells. We infected OVI5E and ES2 cells with a lentivirus expressing an shRNA targeting XPR1 and transplanted these into immunodeficient mice. The growth of these tumor cells was significantly retarded compared to tumor cells infected with control virus (Figure 5). These results suggest that XPR1 is required for the tumorigenicity of OCCC cells in vivo.

In the present study, we identified the transmembrane protein XPR1 as a critical factor in the proliferation and tumorigenicity of epithelial ovarian cancers, especially OCCC. In addition, we observed that XPR1 is upregulated in epithelial ovarian cancers compared to normal tissue. Thus, XPR1 could be a promising molecular target for the therapy of epithelial ovarian cancer. Knockdown of XPR1 leads to the activation of *genes* involved in the *p53* pathway and responses to inflammation and various stresses, including oxidative stress. Knockdown of XPR1 results in the upregulation of *p53* target *genes* such as *PUMA*, *NOXA*, and *GADD45* in *p53* WT cells, but not in

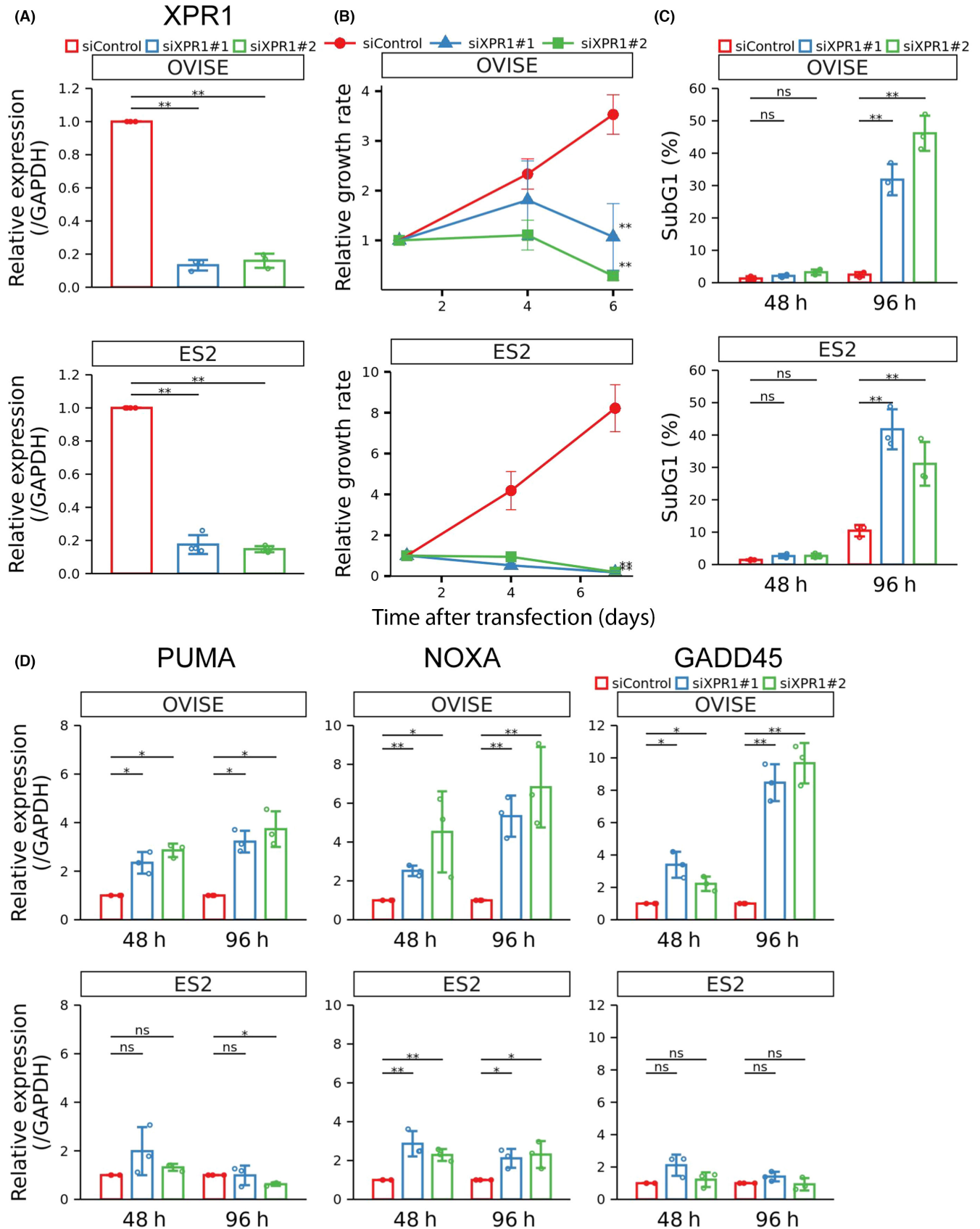


FIGURE 3 Effects of XPR1 knockdown on ovarian clear cell carcinoma (OCCC) cell proliferation and expression of p53 target genes. (A–C) Expression of XPR1 (A), proliferation (B), and sub-G₁ population (C) of OVISE and ES2 cells transfected with siRNAs targeting XPR1 or control siRNA. Results are expressed as the mean \pm SD ($n = 3$). (D) Expression of p53 target genes, PUMA, NOXA, and GADD45, in OVISE and ES2 cells transfected with siRNAs targeting XPR1 or control siRNA. Results are expressed as mean \pm SD ($n = 3$). * $p < 0.05$; ** $p < 0.01$. ns, not significant, unpaired t -test

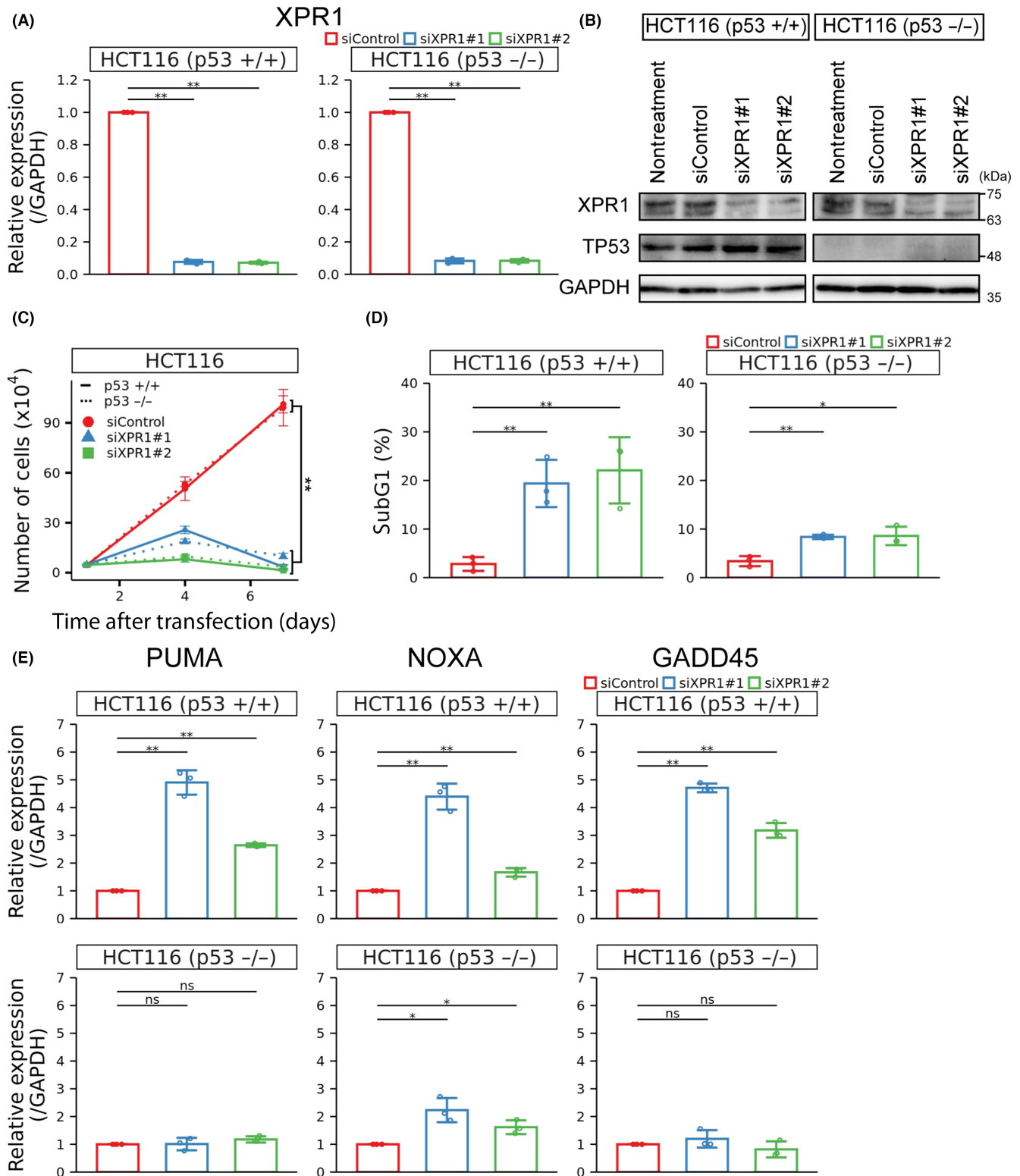


FIGURE 4 Effects of XPR1 knockdown on HCT116 (p53^{+/+}) and HCT116 (p53^{-/-}) cell proliferation and expression of p53 target genes. (A–D) Expression of XPR1 (A, quantitative RT-PCR; B, immunoblotting), the number of viable cells (C), and sub-G₁ population (D) of HCT116 (p53^{+/+}) and HCT116 (p53^{-/-}) cells transfected with siRNAs targeting XPR1 or control siRNA. Results are expressed as the mean \pm SD ($n = 3$). (E) Expression of p53 target genes *PUMA*, *NOXA*, and *GADD45* in HCT116 (p53^{+/+}) and HCT116 (p53^{-/-}) cells transfected with siRNAs targeting XPR1 or control siRNA. Results are expressed as mean \pm SD ($n = 3$). * $p < 0.05$; ** $p < 0.01$. ns, not significant; unpaired t-test

p53-deficient cells. However, XPR1 knockdown induces similar levels of apoptosis in both p53 WT and p53-deficient cells. Thus, XPR1 knockdown-mediated apoptosis can be induced by p53-independent

mechanisms in p53-deficient cells. It has been shown that XPR1 acts as a phosphate exporter and regulates phosphate homeostasis in cooperation with the phosphate importer SLC20A2 in an inositol

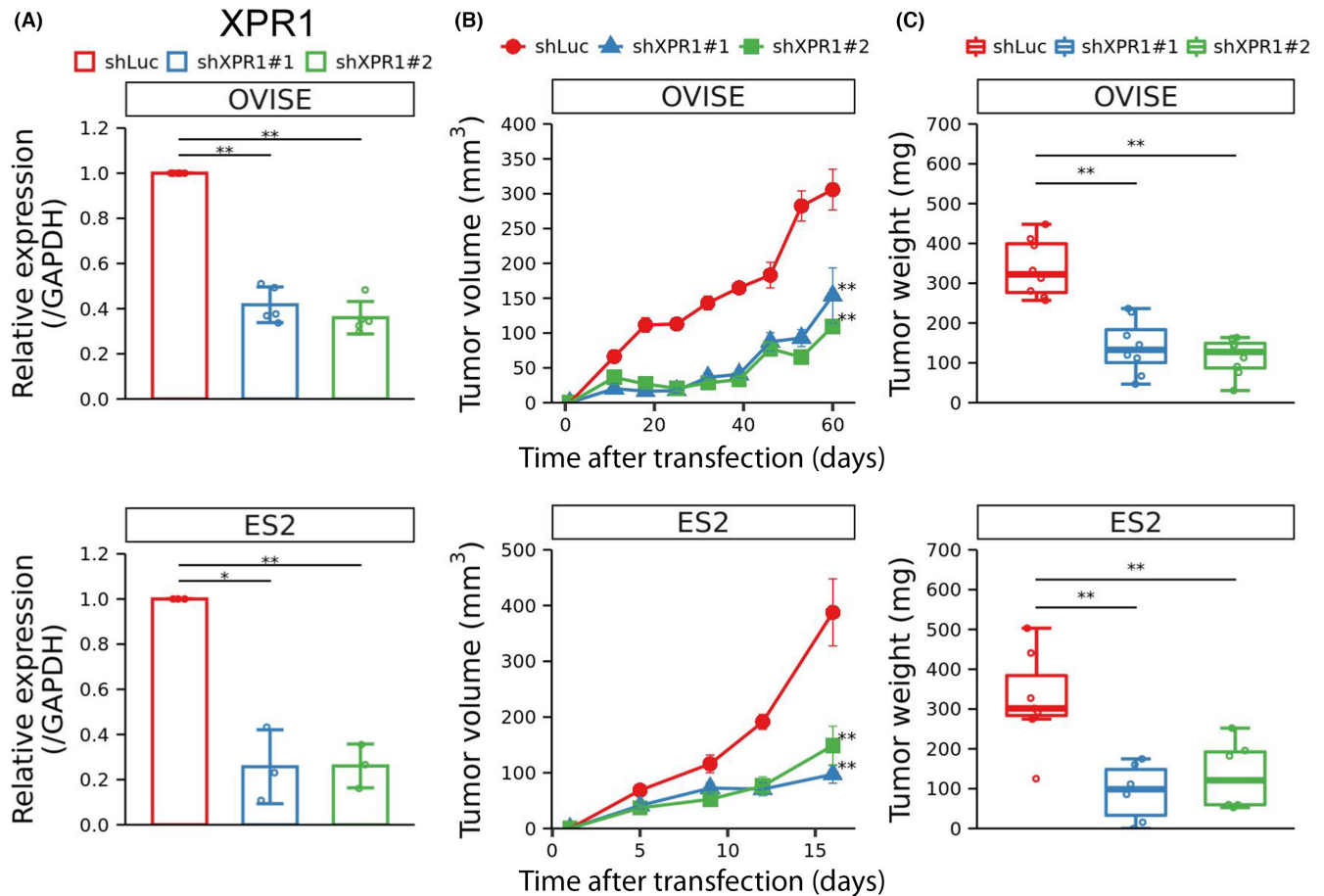


FIGURE 5 XPR1 is required for the tumorigenicity of ovarian clear cell carcinoma (OCCC) cell lines. (A) Quantitative RT-PCR analysis of XPR1 expression in OVISE and ES2 cells transfected with shRNAs targeting XPR1 or negative control shLuc. Results are expressed as the mean \pm SD ($n = 3$). (B, C) OVISE and ES2 cells infected with a lentivirus expressing an shRNA targeting XPR1 or control shRNA were s.c. injected into nude mice ($n = 8$ per group), and tumor volume (B) and tumor weight (C) were measured. Results are expressed as the mean \pm SEM. * $p < 0.05$; ** $p < 0.01$; unpaired t -test

polyphosphate-dependent manner.^{19,20} We speculate that XPR1 knockdown induces p53-dependent and -independent apoptosis by dysregulating phosphate homeostasis. In this regard, it is interesting to note that high extracellular phosphate induces apoptosis along with high levels of intracellular phosphate, reactive oxygen species generation, mitochondrial membrane depolarization, and caspase activation.³⁴ Further investigation is required to clarify the mechanisms underlying apoptosis induced by XPR knockdown.

In conclusion, we have shown that XPR1 is critical for the proliferation and tumorigenicity of epithelial ovarian cancers, especially OCCC. Our results suggest that drugs such as mAbs that inhibit XPR1 function might be useful for the therapeutic treatment of OCCC.

ACKNOWLEDGMENTS

This work was supported by the Project for Cancer Research and Therapeutic Evolution (P-CREATE) no. 17cm0106103h0002, grants from the Japan Agency for Medical Research and Development, and Grants-in-Aid for Scientific Research on Innovative Areas (Integrative Analysis and Regulation of Cellular Diversity, no. 17H06325) from

MEXT, Japan (to TA). This work was also supported by a Grant-in-Aid for Scientific Research (C) (Grant Number 21K07146) from the Japan Society for the Promotion of Science (JSPS), Japan (to TH).

DISCLOSURE

The authors have no conflict of interest. T.A. is an editorial board member of *Cancer Science*.

DATA AVAILABILITY STATEMENT

All raw sequence data (FASTQ format) are deposited in NCBI's Gene Expression Omnibus (GEO) under accession numbers GSE189405 (Figure 1A), GSE189553 (Figure 1C left), and GSE189552 (Figure 2). Code for computational analyses is available from the Lead Contacts, Tetsu Akiyama (akiyama@iqb.u-tokyo.ac.jp) or Tomoatsu Hayashi (hiroton-h@iqb.u-tokyo.ac.jp).

ORCID

Tomoatsu Hayashi  <https://orcid.org/0000-0002-9234-434X>
Tetsu Akiyama  <https://orcid.org/0000-0002-4215-5073>

REFERENCES

- Siegel RL, Miller KD, Fuchs HE, Jemal A. Cancer statistics. *CA Cancer J Clin*. 2022;72:7-33. doi:10.3322/caac.21708
- Matsuda T, Marugame T, Kamo K, et al. Cancer incidence and incidence rates in Japan in 2006: based on data from 15 population-based cancer registries in the monitoring of cancer incidence in Japan (MCIJ) project. *Jpn J Clin Oncol*. 2012;42:139-147.
- Takano M, Kikuchi Y, Yaegashi N, et al. Clear cell carcinoma of the ovary: a retrospective multicentre experience of 254 patients with complete surgical staging. *Br J Cancer*. 2006;94:1369-1374.
- Mizuno M, Kikkawa F, Shibata K, et al. Long-term follow-up and prognostic factor analysis in clear cell adenocarcinoma of the ovary. *J Surg Oncol*. 2006;94:138-143.
- Gilks CB, Ionescu DN, Kalloger SE, et al. Tumor cell type can be reproducibly diagnosed and is of independent prognostic significance in patients with maximally debulked ovarian carcinoma. *Hum Pathol*. 2008;39:1239-1251.
- Iida Y, Okamoto A, Hollis RL, et al. Clear cell carcinoma of the ovary: a clinical and molecular perspective. *Int J Gynecol Cancer*. 2021;31:605-616.
- Ku FC, Wu RC, Yang LY, et al. Clear cell carcinomas of the ovary have poorer outcomes compared with serous carcinomas: results from a single-center taiwanese study. *J9. Formosan Med Assoc*. 2018;117:117-125.
- Tang H, Liu Y, Wang X, et al. Clear cell carcinoma of the ovary clinicopathologic features and outcomes in a chinese cohort. *Medicine*. 2018;97:e10881.
- Crotzer DR, Sun CC, Coleman RL, et al. Lack of effective systematic therapy for recurrent clear cell carcinoma of the ovary. *Gynecol Oncol*. 2007;105:404-408.
- Sugiyama T, Kamura T, Kigawa J, et al. Clinical characteristics of clear cell carcinoma of the ovary: a distinct histologic type with poor prognosis and resistance to platinum-based chemotherapy. *Cancer*. 2000;88:2584-2589.
- Okamoto A, Sehouli J, Yanaihara N, et al. Somatic copy number alterations associated with Japanese or endometriosis in ovarian clear cell adenocarcinoma. *PLoS One*. 2015;10:20116977.
- Itamochi H, Kigawa J, Terakawa N. Mechanisms of chemoresistance and poor prognosis in ovarian clear cell carcinoma. *Cancer Sci*. 2004;99:653-658.
- Jones S, Wang TL, LeM S, et al. Frequent mutations of chromatin remodeling gene ARID1A in ovarian clear cell carcinoma. *Science*. 2010;330:228-231.
- Kuo KT, Mao TL, Jones S, et al. Frequent activating mutations of PIK3CA in ovarian clear cell carcinoma. *Am J Pathol*. 2009;174:1597-1601.
- Battini JL, Rasko JE, Miller AD. A human cell-surface receptor for xenotropic and polytropic murine leukemia viruses: possible role in G protein-coupled signal transduction. *Proc Natl Acad Sci USA*. 1999;96:1385-1390.
- Taylor CS, Nouri A, Lee CG, et al. Cloning and characterization of a cell surface receptor for xenotropic and polytropic murine leukemia viruses. *Proc Natl Acad Sci USA*. 1999;96:927-932.
- Yang YL, Guo L, Xu S, et al. Receptors for polytropic and xenotropic mouse leukaemia viruses encoded by a single gene at Rmc1. *Nat Genet*. 1999;21:216-219.
- Giovannini D, Touhami J, Charnet P, et al. Inorganic phosphate export by the retrovirus receptor XPR1 in metazoans. *Cell Rep*. 2013;3:1866-1873.
- López-Sánchez U, Tury S, Nicolas G, et al. Interplay between PFBC-associated SLC20A2 and XPR1 phosphate transporters requires inositol polyphosphates for control of cellular phosphate homeostasis. *J Biol Chem*. 2020;295:9366-9378.
- Li X, Gu C, Hostachy S, et al. Control of XPR1-dependent cellular phosphate efflux by InsP8 is an exemplar for functionally-exclusive inositol pyrophosphate signaling. *Proc Natl Acad Sci USA*. 2020;117:3568-3574.
- Vaughan AE, Mendoza R, Aranda R, Battini J-L, Millera AD. Xpr1 is an atypical g-protein-coupled receptor that mediates xenotropic and polytropic murine retrovirus neurotoxicity. *J Virol*. 2012;86:1661-1669.
- Legati AG, Giovannini D, Nicolas G, et al. Mutations in XPR1 cause primary familial brain calcification associated with altered phosphate export. *Nat Genet*. 2015;47:579-581.
- Anheim M, López-Sánchez U, Giovannini D, et al. XPR1 mutations are a rare cause of primary familial brain calcification. *J Neurol*. 2016;263:1559-1564.
- Chen WC, Li QL, Pan Q, et al. Xenotropic and polytropic retrovirus receptor 1 (XPR1) promotes progression of tongue squamous cell carcinoma (TSCC) via activation of NF- κ B signaling. *J. Exp Clin Cancer Res*. 2019;38:167.
- Hart T, Tong AHY, Chan K, et al. Evaluation and design of genome-wide CRISPR/SpCas9 knockout screens. *G3: Genes - Genomes - Genetics*. 2017;7:2719-2727.
- Wang B, Wang M, Zhang W, et al. Integrative analysis of pooled CRISPR genetic screens using MAGeCKFlute. *Nat Protoc*. 2019;14:756-780.
- Dobin A, Davis CA, Schlesinger F, et al. STAR: ultrafast universal RNA-seq aligner. *Bioinformatics*. 2013;29:15-21.
- Li B, Dewey CN. RSEM: accurate transcript quantification from RNA-Seq data with or without a reference genome. *BMC Bioinformatics*. 2011;12:323.
- McCarthy DJ, Chen Y, Smyth GK. Differential expression analysis of multifactor RNA-Seq experiments with respect to biological variation. *Nucleic Acids Res*. 2012;40:4288-4297.
- Wu T, Hu E, Xu S, et al. clusterProfiler 4.0: a universal enrichment tool for interpreting omics data. *Innovation*. 2021;2:100141.
- Funato K, Hayashi T, Echizen K, et al. SIRT2-mediated inactivation of p73 is required for glioblastoma tumorigenicity. *EMBO Rep*. 2018;19:e45587.
- Seifert EL, Ligeti E, Mayr JA, et al. The mitochondrial phosphate carrier: role in oxidative metabolism, calcium handling and mitochondrial disease. *Biochem Biophys Res Commun*. 2015;464:369-375.
- Bunz F, Dutriaux A, Lengauer C, et al. Requirement for p53 and p21 to sustain G2 arrest after DNA damage. *Science*. 1998;282:1497-1501.
- Wang S, Wu M, Qin L, Song Y, Peng A. Increased inorganic phosphate induces human endothelial cell apoptosis in vitro. *Am J Physiol Renal Physiol*. 2008;294:F1381-F1387.

SUPPORTING INFORMATION

Additional supporting information may be found in the online version of the article at the publisher's website.

How to cite this article: Akasu-Nagayoshi Y, Hayashi T, Kawabata A, et al. PHOSPHATE exporter XPR1/SLC53A1 is required for the tumorigenicity of epithelial ovarian cancer. *Cancer Sci*. 2022;113:2034-2043. doi:10.1111/cas.15358